Structural and magnetic characterization of oleic acid and oleylamine-capped gold nanoparticles

P. de la Presa, M. Multigner, J. de la Venta, M. A. García, and M. L. Ruiz-González

---

Articles you may be interested in

Ferromagnetism of polythiophene-capped Au nanoparticles
J. Appl. Phys. **109**, 07E328 (2011); 10.1063/1.3562444

Magnetic properties of Aucore-Coshell nanoparticles
J. Appl. Phys. **109**, 07B515 (2011); 10.1063/1.3544493

Magnetism in dodecanethiol-capped gold nanoparticles: Role of size and capping agent
Appl. Phys. Lett. **90**, 213102 (2007); 10.1063/1.2740577

Enhancement of the magnetic anisotropy of Co clusters by Au capping
J. Appl. Phys. **99**, 08G705 (2006); 10.1063/1.2172217

The influence of various coatings on the electronic, magnetic, and geometric properties of cobalt nanoparticles (invited)
J. Appl. Phys. **97**, 10R102 (2005); 10.1063/1.1855191

Structural and magnetic characterization of oleic acid and oleylamine-capped gold nanoparticles

P. de la Presa,[a)] M. Multigner, J. de la Venta, and M. A. García
Instituto de Magnetismo Aplicado (ADIF-UCM-CSIC), P.O. Box 155, Las Rozas, Madrid E-28230, Spain

M. L. Ruiz-González
Departamento Quim. Inorgan., Fac. Quim., Universidad Complutense, Madrid E-28040, Spain

In this work the study of oleic acid and oleylamine-capped gold nanoparticles is presented. The structural characterization of the sample shows 6.7 nm gold nanoparticles with a narrow size distribution. The experimental optical absorption spectrum has a maximum at 2.35 eV. The calculated optical absorption spectrum is shifted and narrower than the experimental one, indicating that the oleic acid and oleylamine do not merely passivate the metallic nanoparticles but modify its electronic structure. These gold nanoparticles show in addition a kind of magnetic order similar to other organic passivated gold nanoparticles as thiol-capped gold nanoparticles. Although the magnetic interactions seem to be weaker than in thiol-capped ones, the magnetic behavior looks similar to that, i.e., an invariant temperature dependence of the magnetization from 5 to 300 K and a noticeable coercive field. We analyze the influence of the organic layer bonding the nanoparticles on the magnetic behavior. © *2006 American Institute of Physics*. [DOI: 10.1063/1.2401314]

I. INTRODUCTION

The inorganic nanoparticles (NPs) protected by organic ligands have attracted much interest due to their divers technological applications.[1–3] The control of the primary structures of nanoparticles, such as size, shape, crystal structure, and composition, is of great importance as they determine the characteristics of nanoparticles including magnetic, electronic, optical, and catalytic properties.

As the size of NPs diminishes, the surface effects become significant and the physical properties of the NPs differ from those of the bulk. To perform systematic investigations of the physical properties, NPs of nearly uniform size and shape are required, therefore, particular attention should be paid to the synthesis methods of particles. The chemical methods like precipitation from solution, coprecipitation, microemulsions, polyols, and high-temperature decomposition of organic precursors have shown to be appropriate to control the size and shape in a rather simple way.[4]

Since Brust and co-workers have reported a synthesis for the preparation of gold nanocrystals passivated with covalently bond alkanethiols,[5] an enormous effort has been done to functionalize these particles with terminally functionalized alkanethiols or arenethiolates as well as polymers,[6] amines,[7] and different organic compounds. Some of these gold functionalized nanoparticles have shown a new kind of magnetic order.

Superparamagnetic behavior has been reported in Pd and Au nanoparticles embedded in poly(N-vinyl-2-pyrrolidone) at low temperatures with a mean diameter of 3 nm,[8] and recently Hori *et al.*[9] have also reported ferromagnetic behavior in Au NPs with protective agents polyacrylonitrile and polyallyl amine hydrochloride (PAAHC-Au). Ferromagnetic spin polarization of Au nanoparticles protected by PAAHC with a mean diameter of 1.9 nm has been measured by x-ray magnetic circular dichroism.[10]

Crespo *et al.*[11] have reported the experimental observation of magnetic hysteresis up to room temperature in dodecanethiol capped Au NPs with 1.4 nm size. On the other hand, Au nanoparticles with similar size but stabilized by a capping agent like tetraoctyl ammonium bromide, which is not covalently bonded but adsorbed by Au atoms, are diamagnetic as bulk Au samples are. The apparent ferromagnetism in thiol-capped NPs is associated with $5d$ localized holes generated through covalent Au-S bonds. These holes give rise to localized magnetic moments that are frozen due to the combination of the high spin-orbit coupling of gold and the symmetry reduction associated with two types of bonding: Au-Au and Au-S.

With the aim to study the magnetic properties induced by organic molecules covalently bonded to gold nanoparticles, the synthesis of Au NPs passivated with oleic acid and oleylamine has been carried out. Structural and magnetic characterizations are performed.

II. EXPERIMENTAL DETAILS

A. Sample preparation

Gold nanoparticles (6.7 nm) were prepared using oleic acid and oleylamine as the capping reagents, which prevent particle aggregation, oxidation, and degradation, as well as render particle surface hydrophobic. In the synthesis 100 mg gold acetate $Au(ac)_3$ 99.9% from Alfa Aesar, 500 mg 1,2-hexadecanediol and 30 ml phenylether was mixed in a three-neck flask fitted with a thermometer, a reflux condenser and an inlet for N_2. The mix was heated up to 80 °C under N_2 atmosphere, then 0.32 ml oleic acid and 0.34 ml oleylamine were added and it was heated to reflux (260 °C). The reflux-

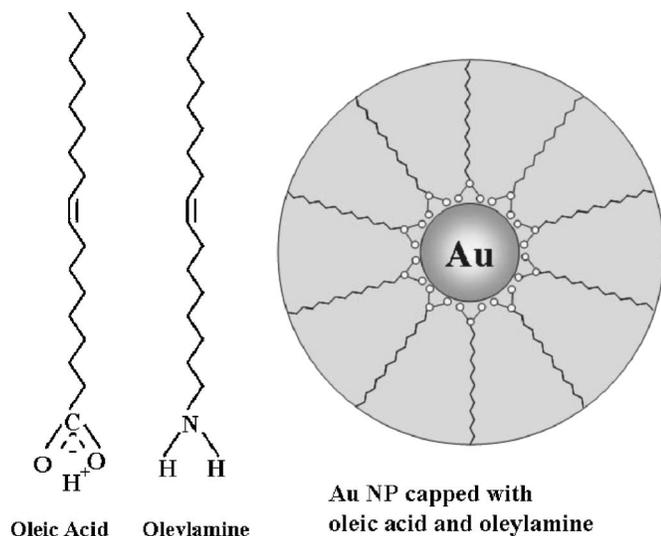[a)]Electronic mail: pdelapresa@adif.es

FIG. 1. Scheme of oleic acid and oleylamine-capped gold NPs.

ing was continued for 30 min. The heat source was then removed, and the reaction mixture was allowed to cool to room temperature. The deep purple product was precipitated by adding ethanol (40 ml) and separated by centrifugation. Yellow-brown supernatant was discarded. The precipitate was dispersed in hexane (25 ml) in the presence of oleic acid (0.05 ml) and oleylamine (0.05 ml). Particles exhibit remarkable long term stability and may even be stored under ambient conditions for days or weeks undergoing no changes. A scheme of the oleic acid and oleylamine-capped gold NPs is shown in Fig. 1.

Since precursor $Au(ac)_3$ contains about 6 ppm of Fe and 2 ppm of Ni, the samples were carefully handled to avoid any extra contamination. To check if any contamination took place during the synthesis, total reflection x-ray fluorescence measurements were performed; nevertheless, due to the small amount of the available sample only an upper limit of 100 ppm was possible to determine.

B. Structural characterization

The particles have been characterized by means of x-ray diffraction (XRD) and transmission electron microscopy (TEM). The XRD pattern can be indexed on the basis of the face-centered-cubic (fcc) Au powder diffraction data. Figure 2 displays a characteristic high-resolution electron micros-
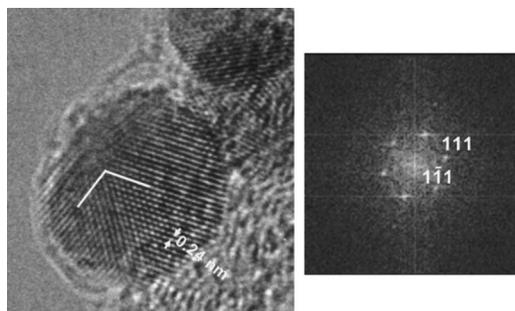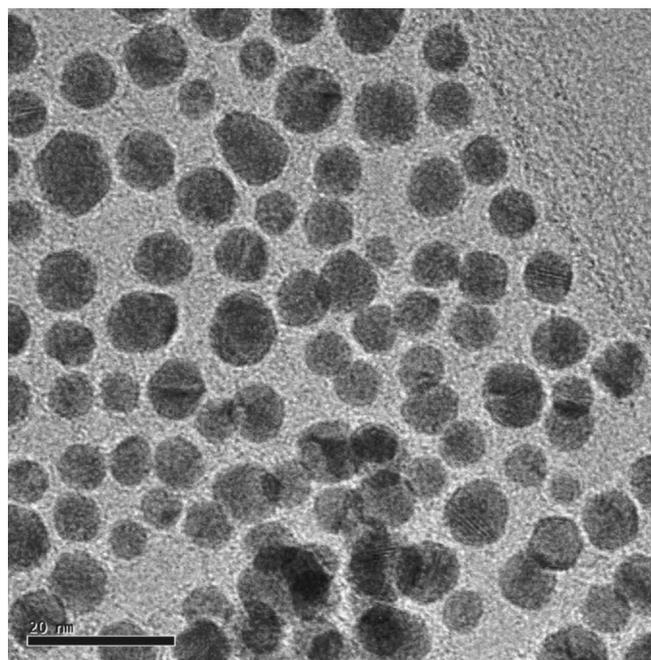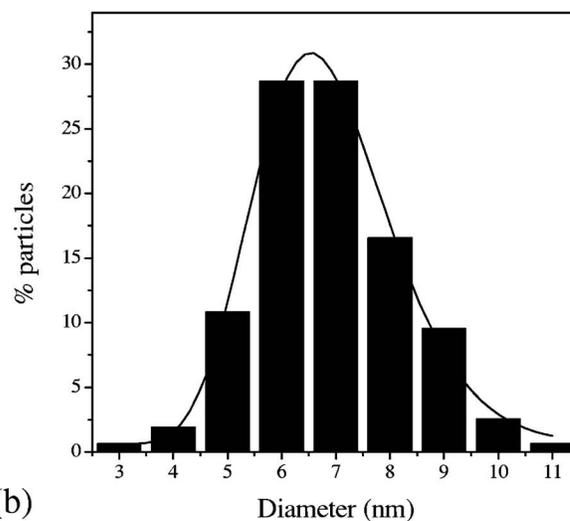

FIG. 2. High-resoltuion TEM image of a Au nanoparticle. The distance between two adjacent planes in Au is 0.24 nm, shown with an arrow. The splitting of the spots due to multiple twinning planes is observed.

FIG. 3. (a) Transmission electron micrographs of oleic acid and oleylamine-capped gold NPs. (b) Particle size distribution histogram, the mean diameter, $d_0 = 6.7$ nm, and the standard deviation, $\sigma = 0.19$ nm.

copy (HREM) image of a gold nanoparticle. The observed periodicites at the image (pointed out in Fig. 2) as well as the corresponding fast Fourier transform are in agreement with the fcc lattice. Moreover, twinned planes are frequently observed, as marked in Fig. 2. A low magnification image is shown in Fig. 3(a), from which the size distribution can be obtained [Fig. 3(b)]. The solid line represents the fit assuming a lognormal distribution, with a mean particle diameter $d_0 = 6.7$ nm and $\sigma = 0.19$ nm.

C. Surface plasmon resonance

Surface plasmon resonance (SPR) is the most remarkable optical property of metallic nanoparticles.[12,13] In the
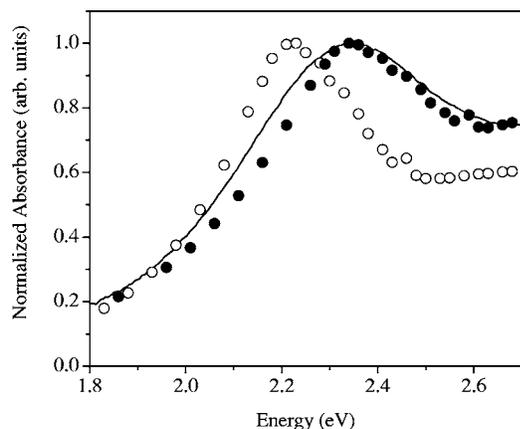
FIG. 4. SPR spectra for oleic acid and oleylamine capped Au NPs (solid line), absorption band according to the Mie theory for NPs with the given size distribution [Fig. 3(b)] and the refractive index of oleic acid ($n=1.44$) (open circle) and the optical absorption spectra for the same size distribution but assuming a localized charge shell with a 1 nm thickness and $n=1.1$ (full circle).

presence of an external electromagnetic field, the conduction electrons oscillate collectively in the NP yielding to an excess of charge at the NP surface that produces a restoring force which tries to re-establish the equilibrium. The movement of the electrons is damped because of their interactions with the NP surface and the atomic core. The whole system acts as a damped oscillator which presents a resonance frequency where the absorption spectrum is maximum. For the most of the transition metals these maxima lie in the ultraviolet-visible part of the spectra.[12,14] When the NPs are spherical and well dispersed (in this case confirmed by HREM measurements) the absorption spectrum corresponding to this resonance can be calculated according to the Mie theory.[12] In the framework of this theory the position of the maximum of the absorption band is determined by the refractive index of the medium surrounding the NPs, while the width is controlled by the particle size.

Figure 4 shows the experimental optical absorption spectra of gold NPs capped with oleic acid and oleylamine, where the maximum appears at 2.35 eV. The optical absorption spectrum calculated for the NPs size distribution of Fig. 3(b) is shifted and narrower than the experimental one (see Fig. 4), indicating that the oleic acid and oleylamine do not merely passivate the metallic NP but modify its electronic structure.[15] It has been shown[16,17] that the capping molecule gives rise to a shell of localized charge (with a thickness around 1 nm) that modifies the refractive index of the medium surrounding the metallic core and reduces the size where the electrons can freely oscillate. Figure 4 shows that a much better agreement between the experiment and the Mie theory is found considering a shell of 1 nm thickness (reducing by 1 nm the size of the NPs measured by HREM) and with a refractive index of 1.1 (clearly different to the value 1.44 corresponding to the oleic acid).

D. Magnetization measurement

Magnetic measurements have been performed using a Quantum Design superconducting quantum interference de-

vice (SQUID) magnetometer. Diamagnetic contributions corresponding to the sample holder system have been previously measured. The total magnetization of the sample is obtained after removing the contribution of the sample holder.

The oleic acid and oleylamine coated Au NPs were synthesized and measured four times to check the reproducibility of the results. However, for the sake of clarity, we illustrate the results of only one of these here.

Figure 5 shows the ferromagnetic behavior of the Au NPs, with a Curie temperature above 300 K. The magnetization is nearly saturated at low temperature by a field of 10 kOe and superparamagnetic behavior is not observed. The saturation remains almost constant from 20 to 300 K. At 5 K there is a noticeable coercive field of about 200 Oe which decreases down to 50 Oe at 300 K. Figure 6(a) displays the thermal dependence of magnetization of Au NPs under a direct current applied field of 500 Oe for 6.7 nm average mean particle size, the magnetization remains almost constant in the whole temperature range.

In order to check the influence of the magnetic impurities of the precursor on the Au NPs, two different samples of the same bottle of $Au(ac)_3$ were characterized (samples I and II): Fig. 6(b) shows the thermal dependence of the magnetization of sample I of $Au(ac)_3$ under a field of 500 Oe; Fig. 7 displays the magnetization curves of both samples at 5 K (curves I and II, respectively). Two different results are observed at 5 K: (i) One of the measurements show an almost diamagnetic behavior (Fig. 7, curve I) although there is also a small ferromagnetic contribution with a coercive field of 500 Oe—that disappears at room temperature—and (ii) on the other hand, sample II behaves nearly paramagnetic (Fig. 7, curve II). The para- or ferromagnetic contributions in samples I and II can be explained by the impurity contain of the precursor $Au(ac)_3$.

III. DISCUSSION

By comparing the results obtained for Au-NPs with those for the precursor $Au(ac)_3$ we find key differences: (i) As can be seen in Fig. 7, curve III, the magnetization at 10 kOe in Au NPs is huge compared with the magnetization produced by the magnetic impurities in $Au(ac)_3$ (Fig. 7, curves I and II), i.e., the presence of magnetic impurities cannot explain of magnetization obtained in gold NPs. (ii) The results obtained for Au NPs are reproducible (four different sample preparations with practically the same results) whereas, on the contrary, the magnetic impurities of $Au(ac)_3$ (see Fig. 7, curves I and II) behave randomly. (iii) The temperature dependence of the magnetization in Au NPs remains constant between 5 and 300 K; on the other hand, in the case of $Au(ac)_3$ the temperature dependence of the magnetization diminishes from 10^{-3} to 10^{-5} emu/g (per gram of gold) in the same temperature range [Figs. 6(a) and 6(b), respectively]. Similar results have been recently reported by Crespo *et al.*,[18] the authors have found that the spontaneous magnetization exhibits a fast decrease with temperature when mag-
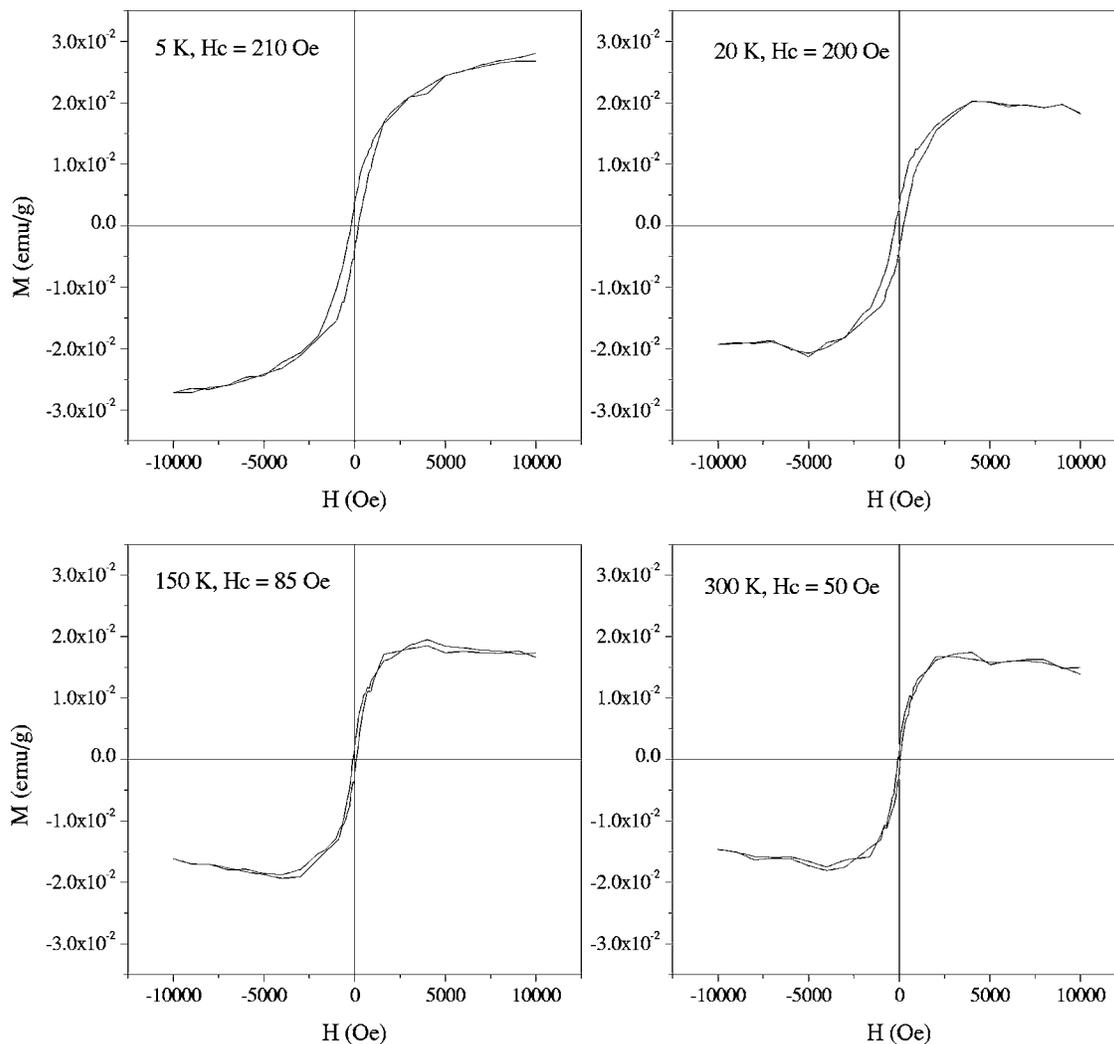
FIG. 5. Magnetization curves of oleic acid and oleylamine-capped gold NPs for $T=5$, 20, 150, and 300 K.

netic impurities are added to gold NPs (in this case Fe NPs) whereas the magnetic hysteresis disappears at room temperature.

These are the most contrasting aspects of the magnetic behaviors of gold NPs and the magnetic impurities. In the case of Au NPs the results are repetitive and reproducible and thermal dependence of the magnetization remains practically constant; on the other hand, the magnetic behavior of the impurities in Au(ac)$_3$ is random and more than one order of magnitude smaller, moreover, the magnetization decreases with temperature when impurities are dominant.

By eye inspecting Fig. 5, it is observed that there is practically no change in the saturation of magnetization of Au NPs from 20 to 300 K, suggesting that the decrease observed between 5 and 20 K is due to the presence of paramagnetic impurities. To show the main contribution to the magnetic order is due to the presence of organic molecules bonding the gold nanoparticles, the sample was heated at 460 °C for 1 h in air. At this temperature the organic molecules are carbonized[7,19] and the nanoparticles grow up to ≈30 nm. After the annealing, the saturation moment is reduced in a ≈90% of the value of the "as prepared" sample (see Fig. 8). The magnetic behavior of the annealed sample

can be attributed to the magnetic impurities contents of the precursors, which could probably cluster due to the thermal annealing.

At 20 K, the magnetization under an applied field of 10 kOe has a value close to 0.02 emu/g(per gram of gold). An estimation of the magnetic moment per gold atoms is straightforward, although the permanent moment is likely associated with an unknown fraction of the total number of atoms (surface or twinned boundary regions). Supposing that those atoms lying on a surface shell of 1 nm thick (estimated from the SPR result) contribute to the magnetic moment, the magnetic moment per Au atom is about 2×10^{-3} μ_B, μ_B being the Bohr magneton. This value is similar to that of PAAHC-Au (Ref. 10) and one order of magnitude smaller than that of dodecanethiol-capped gold nanoparticles.[11] All these magnetic gold nanoparticles have a common condition: the thiol cap, the polymers, the oleic acid, and oleylamine bond covalently to gold atoms. On the other hand, it has been reported[11] that in the case the organic agent is adsorbed instead of covalently bonded, the gold nanoparticles behave as diamagnetic bulk gold.

The size of the nanoparticles seems to play an important role on this kind of magnetism,[11,20] but also the kind and the
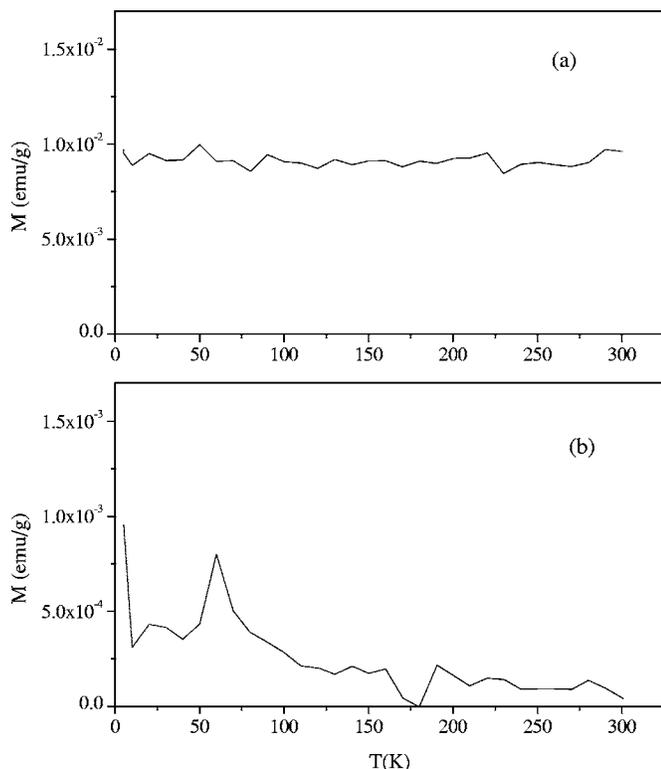
FIG. 6. Temperature variation of the magnetization measured by SQUID magnetometer at 500 Oe for (a) Au NPs and (b) Au(ac)$_3$. The units are emu/g of gold.

length of the organic bonding the nanoparticles.[21] In contrast to the polymers, where the length and the number of chains bonded to the surface atoms of gold NPs cannot be determined at all, in the dodecanethiol capped gold NPs,[11] each 12 CH$_2$ chain is bonded to Au atoms via the Au-S covalent bond and thus can be compared to the oleic acid and oleylamine capped gold NPs.

The chemical behavior and stability of the oleic acid and oleylamine-capped gold NPs are similar to that of their thiol-
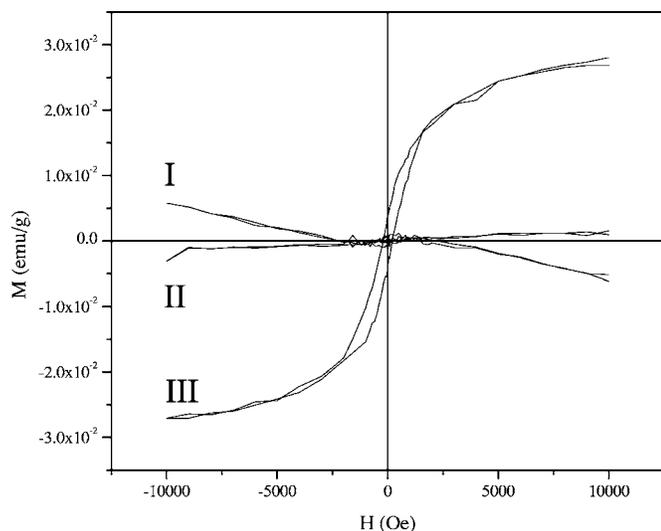

FIG. 7. Magnetization at 5 K of two different measurements of the precursor Au(ac)$_3$ (curves I and II) and oleic acid and oleylamine-capped gold NPs (curve III). The units are emu/g of gold.
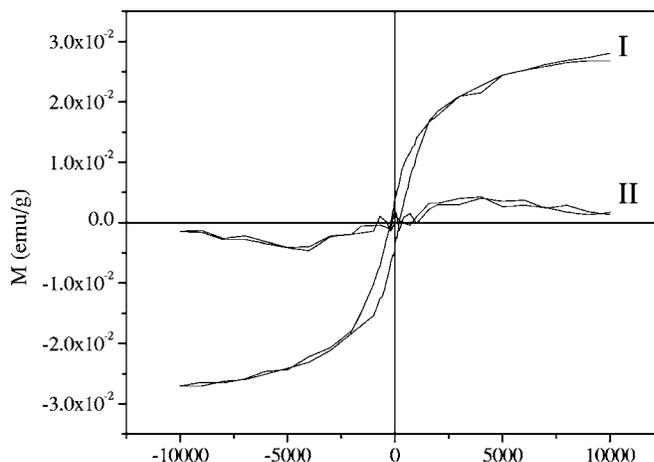

FIG. 8. Magnetic response of the as prepared (curve I) and the annealed Au NPs (curve II). The thermal annealing was at 460 °C during 1 h.

capped counterparts, although the first poses an 18-CH2 chain cap instead of 12 or 9–CH2. The main differences lie in the strength of the covalent bond and the stability. The strength of the covalent bond is in some way related to the difference of the electronegativity of two bonded atoms, i.e., Au-S (thiol cap), Au-N (amine cap), and Au-O (oleic acid cap), so that the smaller the difference, the stronger the covalent bond. Then, the Au-O bond is the weakest of the three and will be not at first considered.

The chemical and physical characteristics concerning the bonding mode of the oleylamine surface passivants are consistent with a charge neutral amine/gold surface interaction described by a weak covalent bond. Differential scanning calorimetry measurements on various Au nanocrystals[7] indicate that the Au-N interaction is weaker than the Au-S interaction. On the other hand, the stability of amine-capped Au nanocrystals is a finite-size effect which is largely kinetic, rather than thermodynamic, in origin. This contrasts with the system of thiol-capped Au nanocrystals, which possess thermodynamic stability with respect to ligand desorption and subsequent particle agglomeration.

Let us assume that the origin of the magnetic order observed in the oleic acid and oleylamine-capped gold NPs is very similar to that of their thiol-capped gold counterpart. In the case of thiol-capped one, the Au-S covalent bond is stronger and the relationship of the surface to the core electrons is greater than in the amine case because of the smaller size of the former, leading to a negligible diamagnetic contribution. This could induce one to think that in the amine case the magnetic order should be negligible. On the other hand, Ichii *et al.*[22] have measured the surface potential by noncontact atomic force microscopy in thiol-capped gold films and have found that the voltage increases linearly with the chain length at a rate of 9 mV per CH$_2$. This contact potential is related to the strength of the charge transfer between the organic layer and the metal and it has been shown that the observed magnetism is accounted for by this charge transfer.[21] In the case of oleic acid and oleylamine-capped Au NPs the organic chain is 50 % longer than in dodecanethiol-capped ones, which could lead to a higher contact potential acting on the surface atoms. Besides that,

there is also a significant amount of twinned planes, as can be seen in Fig. 2, which are an important source of charges. These two facts, a longer CH_2 chain and the significant amount of twinned planes, can lead to the observation of ferromagnetic-like behavior in spite of the size of the NPs.

An explanation of the physics behind of this "ferromagnetic-like behavior" has recently been given by Hernando *et al.*[23] The authors have argued that the combination of spin-orbit coupling and contact potential at the large radius domain boundaries can account for the existence of giant orbital moment induced in atomic-like localized states. The contact potential is originated by electron holes induced by electron transfer to the organic molecule. Electrostatic interaction between electrons trapped in the orbital yields spin alignment that, through spin-orbit coupling, induces subsequent orbital moment alignment. This argument can also be extended to other sources of broken symmetry like twin boundaries.

IV. SUMMARY

In conclusion, we have synthesized gold nanoparticles coated with oleic acid and oleylamine of about 6.7 nm and a narrow size distribution. The HREM image of a gold nanoparticle shows the structure corresponding to fcc structured Au and, moreover, multiple twinned planes. The calculated optical absorption spectrum is narrower than the experimental one, indicating that the oleic acid and oleylamine do not merely passivate the metallic NP but modify its electronic structure. The covalent bond of the organic molecules to the gold atoms of the surface induces a ferromagnetic-like behavior of the NPs similar to that of the thiol-capped counterparts which features are an invariant temperature dependence of the magnetization from 5 to 300 K and a noticeable coercive field.

ACKNOWLEDGMENTS

[1] S. Sun, C. B. Murray, D. Weller, L. Folks, and A. Moser, Science **287**, 1989 (2000).
[2] P. V. Kamat, J. Phys. Chem. B **106**, 7729 (2002).
[3] C. C. Berry and A. S. G. Curtis, J. Phys. D **36**, R198 (2003).
[4] P. Tartaj, M. P. Morales, S. Veintemillas-Verdaguer, T. González-Carreño, and C. J. Serna, J. Phys. D **36**, R182 (2003).
[5] M. Brust, M. Walker, D. Bethell, D. J. Schiffrin, and R. J. Whyman, J. Chem. Soc., Chem. Commun. **1994**, 801 (1994).
[6] T. Teranishi, I. Kiyokawa, and M. Miyake, Adv. Mater. (Weinheim, Ger.) **10**, 596 (1998).
[7] D. V. Leff, L. Brandt, and J. R. Heath, Langmuir **12**, 4723 (1996).
[8] H. Hori, T. Teranishi, Y. Nakae, Y. Seino, M. Miyake, and S. Yamada, Phys. Lett. A **263**, 406 (1999).
[9] H. Hori, Y. Yamamoto, T. Iwamoto, T. Miura, T. Teranishi, and M. Miyake, Phys. Rev. B **69**, 174411 (2004).
[10] Y. Yamamoto *et al.*, Phys. Rev. Lett. **93**, 116801 (2004).
[11] P. Crespo *et al.*, Phys. Rev. Lett. **93**, 087204 (2004).
[12] U. Kreibig and M. Völlmer, *Optical Properties of Metal Clusters* (Springer-Verlag, Berlin, 1995).
[13] H. Hövel, S. Fritz, A. Hilger, U. Kreibig, and M. Völlmer, Phys. Rev. B **48**, 18178 (1993).
[14] J. A. Creighton and D. G. Eadon, J. Chem. Soc., Faraday Trans. **87**, 3881 (1991).
[15] I. L. Garzón *et al.*, Phys. Rev. Lett. **85**, 5250 (2000).
[16] A. C. Templeton, J. J. Pietron, R. W. Murray, and P. Mulvaney, J. Phys. Chem. B **104**, 564 (2000).
[17] M. A. García, J. de la Venta, P. Crespo, J. LLopis, S. Penadés, A. Fernández, and A. Hernando, Phys. Rev. B **72**, 241403(R) (2005).
[18] P. Crespo, M. A. García, E. Fernández, M. Multigner, D. Alcántara, J. M. de la Fuente, S. Penadés, and A. Hernando, Phys. Rev. Lett. **97**, 177203 (2006).
[19] V. Pérez-Dieste *et al.*, Appl. Phys. Lett. **83**, 5053 (2003).
[20] P. Zhang and T. K. Sham, Phys. Rev. Lett. **90**, 245502 (2003).
[21] I. Carmeli, G. Leitus, R. Naaman, S. Reich, and Z. Vager, J. Chem. Phys. **118**, 10372 (2003).
[22] T. Ichii, T. Fukuma, H. Yamada, and K. Matsushige, Nanotechnology **15**, s30 (2004).
[23] A. Hernando, P. Crespo, and M. A. García, Phys. Rev. Lett. **96**, 057206 (2006).